

Full -Scale Validation of the Wind-Induced Response of Tall Buildings: Updated Findings from the Chicago Monitoring Project

Tracy Kijewski-Correa^{1*}, John Kilpatrick², Dae-Kun Kwon³, Rachel Bashor⁴, Bradley S. Young⁵, Ahmad Abdelrazaq⁶, Jon Galsworthy⁷, Dave Morrish⁸, Robert C. Sinn⁹, William F. Baker¹⁰, Nick Isyumov¹¹, Ahsan Kareem¹²

¹ Assistant Professor, University of Notre Dame, Notre Dame, IN, USA, tkjewsk@nd.edu

² Graduate Student, Boundary Layer Wind Tunnel, University of Western Ontario, London, Ontario, Canada, jkilpatr@uwo.ca

³ Research Associate, University of Notre Dame, Notre Dame, IN, dkwon@nd.edu

⁴ Graduate Student, University of Notre Dame, Notre Dame, IN, rstansel@nd.edu

⁵ Engineer, Skidmore Owings and Merrill LLP, Chicago, IL, USA, bradley.young@som.com

⁶ Vice President, Samsung corporation, Engineering and Construction Group, Korea, ahmad.abdelrazaq@samsung1.com

⁷ Assistant Professor and Associate Research Director, Boundary Layer Wind Tunnel, University of Western Ontario, London, Ontario, Canada, jg@blwtl.uwo.ca

⁸ Computer Systems Analyst, Boundary Layer Wind Tunnel, University of Western Ontario, London, Ontario, Canada, dpm@blwtl.uwo.ca

⁹ Associate Partner, Skidmore Owings and Merrill LLP, Chicago, IL, USA, robert.c.sinn@som.com

¹⁰ Partner, Skidmore Owings and Merrill LLP, Chicago, IL, USA, william.f.baker@som.com

¹¹ Research Consultant, Boundary Layer Wind Tunnel, University of Western Ontario, London, Ontario, Canada, ni@blwtl.uwo.ca

¹² Professor, University of Notre Dame, Notre Dame, IN, USA, kareem@nd.edu

ABSTRACT

While high-rise construction serves as one of the most challenging projects undertaken by society each year, tall buildings are one of the few constructed facilities whose design relies solely upon analytical and scaled models, which, though based upon fundamental mechanics and years of research and experience, has yet to be systematically validated in full-scale. In response to this deficiency, a full-scale monitoring project was initiated through the combined efforts of members of academe (University of Notre Dame), a design firm (Skidmore, Owings and Merrill, Chicago) and a wind tunnel laboratory (Boundary Layer Wind Tunnel Laboratory, University of Western Ontario). The objective of this program is to monitor the full-scale response of three tall buildings in Chicago and compare this to the predictions from wind tunnels and finite element models used in their design, suggesting changes where appropriate to refine the design state-of-the-art. This also includes an evaluation of the in-situ periods and damping ratios over a range of response amplitudes. This paper overviews the research project, current status of activities and presents updated findings of the program.

KEYWORDS: Wind Tunnel Testing, Damping, Full-Scale Monitoring, High-Rise Design

INTRODUCTION

Even though the performance of tall buildings affects the safety and comfort of a large number of people in both residential and office environments, tall buildings are one of the few constructed facilities whose design relies solely upon analytical and scaled models, which, though based upon fundamental mechanics and years of research and experience, has yet to be systematically validated in full-scale. In particular, as state-of-the-art structural analysis software and wind tunnel testing are advancing rapidly,

* Corresponding author. Tel.: 574-631-2980; fax: 574-631-9236

Mailing address: 156 Fitzpatrick Hall, Notre Dame, IN, 46556, USA.

the accuracy and validity of their results needs to be calibrated with respect to actual performance. Understandably, since the development of full-scale models for this type of structure is not feasible, monitoring the performance of actual structures becomes the most viable means for verification and improvement of current design practices and analytical modeling approaches. The latter becomes particularly important to insure satisfactory performance, economy and efficiency of future designs with increased complexity and height. Though monitoring has now become commonplace in seismic zones in the United States, the tall buildings community has unfortunately not followed suit.

In response to this need, a partnership between the University of Notre Dame (UND), the Boundary Layer Wind Tunnel Laboratory (BLWTL) at the University of Western Ontario (UWO) and Skidmore, Owings & Merrill LLP (SOM) in Chicago was established to initiate the Chicago Full-Scale Monitoring Program. Through the program, the actual performance of three tall buildings in Chicago is compared to predictions, both by finite element and wind tunnel models, thereby providing an important missing link between analytical modeling and actual behavior. Based on these comparisons, sources of discrepancies are identified to allow enhancement of current design practice. These evaluations also examine the in-situ periods and damping ratios of the buildings under a variety of wind conditions and over a range of response amplitudes. As such, these efforts will enhance existing databases presently lacking substantial information on buildings of significant height.

DESCRIPTION OF INSTRUMENTED BUILDINGS

The primary objective of this study is to correlate the in-situ measured response characteristics of tall buildings in full-scale with computer-based analytical and wind tunnel models for the advancement of the current state-of-the-art in tall building design. Such an endeavor requires the selection of several buildings representative of structural systems common to high-rise design, all located in the same general locale of downtown Chicago, for which design information and building access are obtainable. Since major effort was expended to establish relationships with the building owners to allow access, the anonymity of the buildings must be assured to guarantee continued access for the life of the program. As such, the structures will be generically referenced as Buildings 1, 2, and 3. A brief description of noteworthy features of each building's structural system is now provided:

Building 1: The primary lateral load-resisting system features a steel tube comprised of exterior columns, spandrel ties and additional stiffening elements to achieve a near uniform distribution of load on the columns across the flange face, with very little shear lag.

Building 2: In this reinforced concrete building, shear walls located near the core of the building provide lateral load-resistance. At two levels, this core is tied to the perimeter columns via reinforced concrete outrigger walls to control the wind drift and reduce overturning moment in the core shear walls.

Building 3: The steel moment-connected, framed tubular system of Building 3 behaves fundamentally as a vertical cantilever fixed at the base to resist wind loads. The system is comprised of closely-spaced, wide columns and deep spandrel beams along multiple frame lines.

As each building is rectangular in plan, with the primary axes aligning with North and East, subsequent discussions will reference sway response as North-South (N-S) or y-sway and East-West (E-W) or x-sway for simplicity, as shown in Figure 1.

INSTRUMENTATION OVERVIEW

Each building is equipped with the same primary instrumentation system that features four Columbia SA-107 LN high-sensitivity force balance accelerometers mounted in orthogonal pairs at two opposite corners of the ceiling at the highest possible floor in each building, as shown in Figure 1. The outputs of these sensors are sampled every 0.12 seconds and archived by a 15-bit Campbell CR23X data logger. The primary instrumentation systems were respectively installed in Buildings 1, 2 and 3 on 06/14/02, 6/15/02 and 4/30/03. Though wind-induced displacements are characterized by both background (quasi-static) and resonant components, only the latter can be recovered by the aforementioned accelerometer system. Therefore, it was of interest to monitor both of these contributions in full-scale using Global Positioning

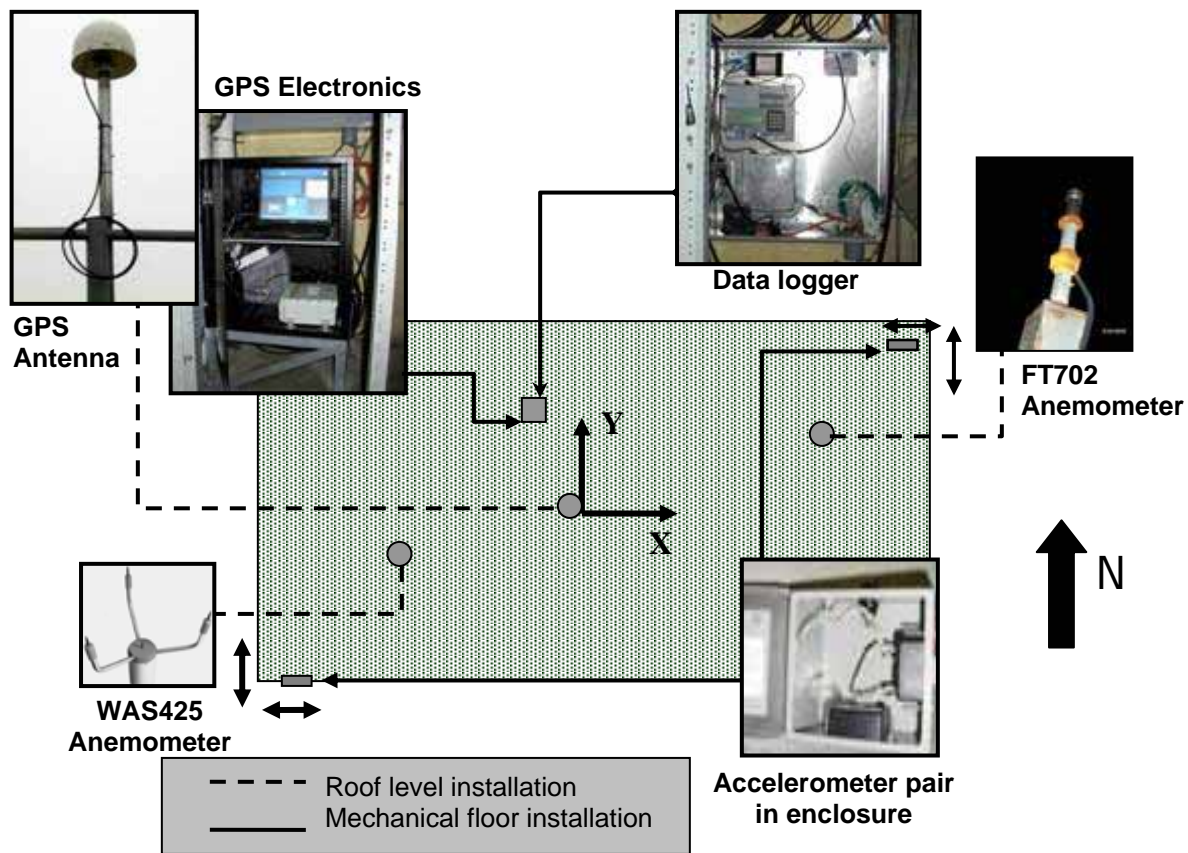


Figure 1. Generalized sensor array on generic floor plan with inset photographs of equipment.

Systems (GPS). A differential GPS sensor pair was installed at the centerline of Building 1 and on a nearby stationary reference building on 8/26/02. In this differential configuration, the Leica MC 500 GPS used in this study are capable of achieving sub-centimeter resolution, based on calibrations conducted before full-scale deployment [1].

In addition, two ultrasonic anemometers were installed on masts 41 m above the rooftop of the tallest building in the program, Building 3, so that the reference wind speed and direction for each event may be measured at this site and reliably converted to represent the wind speed at the top of each instrumented building. This installation was completed in the summer of 2004. An interim wind monitoring protocol was established, while the final installation of these anemometers was coordinated at Building 3. This interim data is collected at a NOAA GLERL meteorological station in Lake Michigan, elevated 75 feet above lake level and located 3 miles offshore of downtown Chicago. These data are extrapolated to gradient (taken as 300 m over open water) using methods to account for the influence of terrain roughness and fetch [2].

WIND TUNNEL TESTING

Though aeroelastic model tests would provide direct information on aerodynamic damping effects and, depending on the type of model, contributions of higher modes of vibration to the response, the high-frequency force-balance (HFFB) method was chosen for the wind tunnel tests in this study as it allows the flexibility to repeat response predictions based on the measured modal force spectra but considering different building dynamic properties without the requirement of additional wind tunnel testing. Accordingly, differences between the in-situ and predicted structural properties of the buildings are easily

reconciled using the HFFB method as compared to aeroelastic tests. The modeling for the force balance tests conducted in this study consisted of three components: 1) a rigid and lightweight detailed 1:500 scale model of each of the study buildings; 2) a detailed model of the structures surrounding the building sites within a full-scale radius of about 750 m; and 3) a less detailed model of the upstream terrain, chosen to simulate the scaled turbulence intensity and velocity profiles expected at full-scale for each site. All wind tunnel tests were conducted in the high-speed section of the closed-circuit wind tunnel (BLWT II) at the BLWTL at UWO. The length of the high-speed section of the tunnel is approximately 38.5m, and the dimensions of the tunnel at the test section are 4.5m x 2.5m (width by height). The top speed of the wind tunnel is approximately 27 m/sec, measured at the entrance of the high-speed test section.

The velocity and turbulence intensity profiles used for the model scale tests of the three buildings in this study were based primarily on a categorization of the terrain surrounding the sites and the Engineering Sciences Data Unit (ESDU). The roughness length values and the associated terrains assumed in the profile development are provided in Table 1. Typical velocity and turbulence profiles developed during the wind tunnel studies are presented in Figure 2.

Table 1. Terrain and Surface Roughness Lengths Assumed for Profile Development.

Terrain description	Effective roughness length z_o (m)
Water/lake	0.0022 - 0.0043 ^a
Open	0.03
Suburbs/outskirts of city	0.3 - 0.5
Urban/city center	1.0 - 3.0

^a Roughness length over water is estimated as a function of the local friction velocity (after ESDU 01008).

Each building was tested at 10° increments for the full 360° azimuth range. Time histories of the responses, as well as the mean and RMS base bending and torsional moments were recorded, and their associated power spectra were subsequently obtained. The generalized forces acting on the building in the sway directions are related to the base moments through approximately linear mode shapes $\phi(z)$, with a 0.7 correction factor for torsion. The generalized force in mode j at each time increment is:

$$F_j^*(t) = \int_0^H f_x(z,t)\phi_{xj}(z)dz + \int_0^H f_y(z,t)\phi_{yj}(z)dz + \int_0^H f_\theta(z,t)\phi_{\theta j}(z)dz \quad (1)$$

where

$$\int_0^H f_x(z,t)\phi_{xj}(z)dz \approx \int_0^H f_x(z,t)a_{xj}\left(\frac{z}{H}\right)dz = \frac{a_{xj}}{H}M_x(t) \quad \int_0^H f_y(z,t)\phi_{yj}(z)dz \approx \int_0^H f_y(z,t)a_{yj}\left(\frac{z}{H}\right)dz = \frac{a_{yj}}{H}M_y(t) \quad (2 \text{ a-c})$$

$$\int_0^H f_\theta(z,t)\phi_{\theta j}(z)dz \approx 0.7a_{\theta j}T(t)$$

where $M_x(t)$, $M_y(t)$ and $T(t)$ are the base moments in x, y and torsion, and a_{xj} , a_{yj} , and $a_{\theta j}$ are the modal mixing factors. Note that corrections [3] to adjust for non-linear mode shapes are applied to obtain improved estimates of the generalized forces for prediction of building accelerations. Using the above formulations, the generalized force in mode j at each time increment can be written in terms of the measured base moments as

$$F_j^*(t) = \frac{a_{xj}}{H}C_{xj}M_x(t) + \frac{a_{yj}}{H}C_{yj}M_y(t) + 0.7a_{\theta j}C_{\theta j}T(t) \quad (3)$$

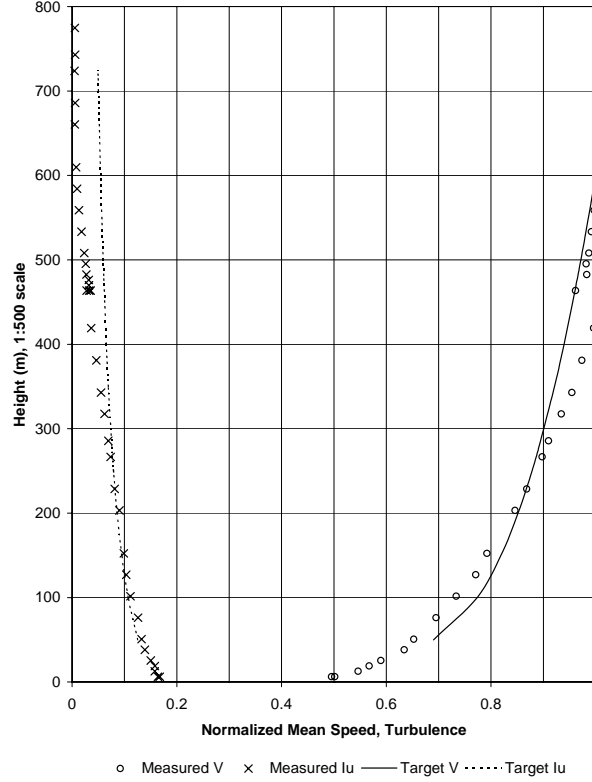


Figure 2. Simulated mean wind speed (O) and turbulence intensity (x) profiles with solid and dashed lines indicating target profiles, respectively.

where C_{xj} , C_{yj} and C_{zj} are the mode shape corrections. In the HFFB method, the responses of the buildings are typically described by the dynamic responses in the first three fundamental modes of vibration.

The resulting RMS acceleration along the building's x-axis at any height z_{acc} above grade due to the generalized force acting in mode j may be written as follows:

$$\sigma_{\ddot{x}_j} = (2\pi f_j)^2 \frac{\sigma_{F_j^*}^2}{K_j^*} \phi_{xj}(z_{acc}) \sqrt{\frac{\pi}{4\zeta_j} \frac{f_j S_{F_j^*}(f_j)}{\sigma_{F_j^*}^2}} \quad (4)$$

where f_j is the natural frequency in mode j , $\sigma_{F_j^*}^2$ is the variance of the generalized force in mode j , K_j^* is the generalized stiffness in mode j , $S_{F_j^*}(f_j)$ is the value of the power spectral density of the generalized force at the natural frequency, and ζ_j is the structural damping in mode j . Accelerations in the y-axis and torsional directions are similarly defined. The maximum acceleration in the x-direction is comprised of the components acting in modes $j=1..3$, which are combined using the complete quadratic combination (CQC) method as follows:

$$\sigma_{\ddot{x}} = \sqrt{\sum_i \sum_j \sigma_{\ddot{x}_i} \rho_{ij} \sigma_{\ddot{x}_j}} \quad (5)$$

where $\sigma_{\ddot{x}_i}$ and $\sigma_{\ddot{x}_j}$ are the modal accelerations in the x-axis in modes i and j , and ρ_{ij} is the modal cross-correlation coefficient. For well separated frequencies, the cross-correlation coefficient ρ_{ij} approaches 0, and the total acceleration in the x-direction may be written simply as the sum of the root-sum of squares (SRSS) of the acceleration components in modes 1 through 3. Note that more advanced modal combination procedures have recently been proposed in Chen and Kareem [4], which are particularly

valuable for buildings with closely spaced frequencies. However, due to the rather modest level of coupling, the results may not be significantly affected when compared to other sources of uncertainty, e.g., estimates of gradient wind speeds from surface level winds.

FINITE ELEMENT MODELING

For the buildings associated with this study, finite element models were developed using currently available commercial software: ETABS [5] and SAP 2000 [6], based upon careful reference to the design drawings. It was not the purpose of this study to apply a unique set of modeling assumptions to the FE models in order to mimic a known, in-situ measured result. Rather, all assumptions regarding the finite element representation of the buildings in this study reflect those commonly applied in design offices for serviceability assessment.

For Buildings 1 and 3, framed primarily in structural steel, the representation of the member stiffness was straight-forward, as the steel elements remain elastic at service level loadings. For the reinforced concrete building (Building 2), adjustments were made to selected lateral-load resisting elements to represent the post-cracking stiffness of these elements under service level loads. Specifically, the flexural and shearing stiffnesses of the link (coupling) beams within the shear wall system were reduced to one-half and one-fifth of the elastic stiffness, respectively. The beam-supported slab was modeled using shell elements. The flexural stiffness of the slab's shell elements was set to one-half of the elastic stiffness in order to approximate the post-cracking behavior of the slab, which transfers flexure and shear between the perimeter columns and core shear walls. While generally considered to support gravity floor loads alone, explicit modeling of the linkage between the floors, exterior columns, and core often results in a substantial contribution to lateral resistance in reinforced concrete buildings.

Figure 3 shows the mode shapes for each of the buildings, normalized with respect to the top floor displacement. The inset in each figure shows the axes of vibration displayed in the plot. Table 2 summarizes the resulting periods from the FE analyses conducted at SOM and the damping levels assumed by the original designers of the buildings. Buildings 2 and 3 undergo coupled responses, though the extent of coupling in Building 2 is much less than Building 3. Note that although the authors acknowledge that Building 2 can be reasonably expected to have higher damping, the damping values of 1% for habitability/serviceability and 1.5% for survivability reported in Table 2 were the values specified in their design.

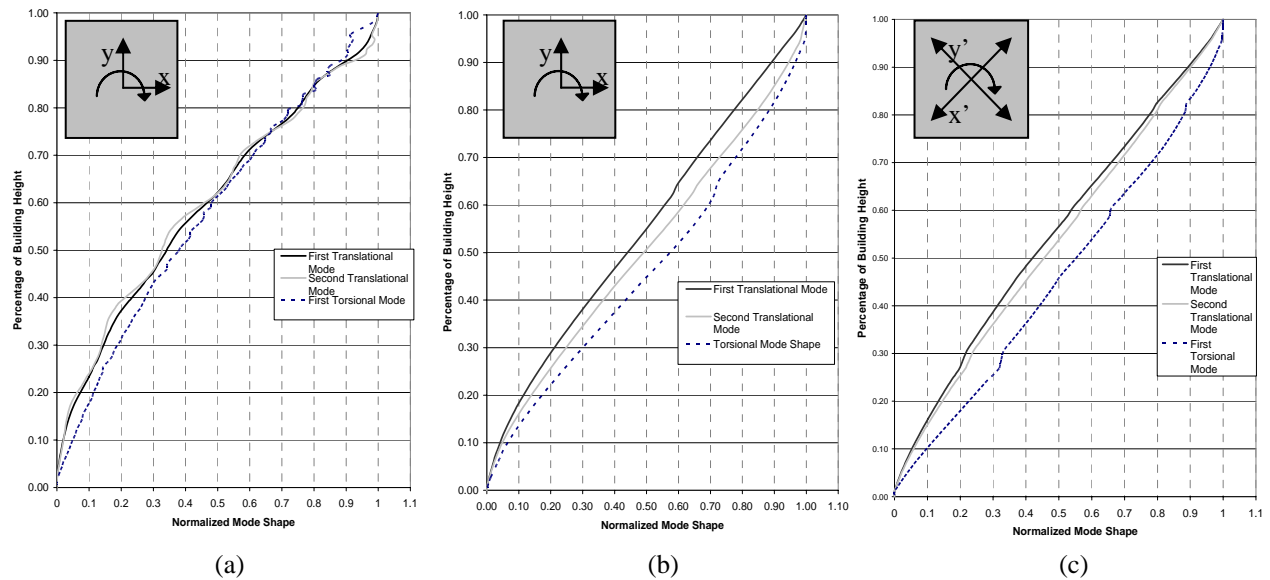
Table 2. Periods of Vibration and Assumed Damping Levels for Finite Element Models of Buildings 1-3.

	Mode 1		Mode 2		Mode 3	
	Period	Damping	Period	Damping	Period	Damping
Building 1	<i>Y-axis translation</i> 7.0 s	1%	<i>X-axis translation</i> 4.9 s	1%	<i>Torsion</i> 2.0 s	1%
Building 2	<i>X-axis translation, slight torsion</i> 6.7 s	1%*	<i>Y-axis translation, slight torsion</i> 6.4 s	1%*	<i>Coupled Torsion</i> 4.6 s	1%*
Building 3	<i>Fully coupled x-translation</i> 7.7 s	1%	<i>Fully coupled y-translation</i> 7.6 s	1%	<i>Fully coupled torsion</i> 4.5 s	1%

*1% used for accelerations, 1.5% used for base moments.

DATA INVENTORY

A total of over 8000 hours of time histories have been collected thus far in the program. During this monitoring period, numerous wind events have been observed with mean hourly surface-level wind



speeds exceeding 18 m/s, many associated with the windiest spring on record for the City of Chicago since 1991. In fact, during March and April of 2004, 11 “damaging wind speed” events were recorded [7].

Figure 3. Normalized fundamental mode shapes for Buildings (a) 1, (b) 2 and (c) 3.

EXAMPLE RESPONSE ANALYSIS

An example of the measured response of all three buildings for the April 28-29, 2004 wind event is now presented. A second data sampling for Building 1 during the February 11, 2003 wind event was presented in Kilpatrick et al. [8]. For the following discussion, wind field characteristics are described by the output of the NOAA GLERL sensor. Mean hourly wind speed from the NOAA sensor is shown in Figure 4a and is extrapolated to gradient level by two methods. Method 1 involves the use of power law expressions, coefficients and gradient heights readily available in ASCE 7-02 [9] (Fig. 4b). Method 2, shown in Figure 4c, uses the interim wind protocol discussed previously in the Instrumentation Overview section. The surface level wind directions are provided in Figure 4d. A comparison of Figures 4b and 4c demonstrates a good agreement between methods conventionally used by commercial wind tunnel testing facilities (Method 2, Fig. 4c) and those standardized in ASCE 7 (Method 1, Fig. 4b).

EXTRACTED DYNAMIC PROPERTIES

To determine the natural frequency and damping of the three buildings under ambient vibrations, two system identification (SI) techniques assuming white noise inputs were utilized, a power spectral approach using the Half-Power Bandwidth Technique (HPBW) [10] and the Random Decrement Technique (RDT) [11]. As both approaches invoke assumptions of stationarity, three separate stationarity tests were performed to investigate the validity of this assumption for the April 28-29 wind event. These tests included the Run and Reverse Arrangements Tests [10] and a method proposed by Montpelier [12]. It was determined that passing at least two of the stationarity tests was sufficient, leading to the following respective success rates for each of the buildings: 95.2%, 77.8%, and 91.7%. Records satisfying these conditions were then used in the aforementioned system identification analyses.

Spectral Analysis: Given the narrowbanded nature of the buildings in this study, the simultaneous reduction of bias and variance errors can be quite challenging, given the limited amount of data satisfying the stationarity checks conducted here. In light of this, spectral damping is generally overestimated and can have significant uncertainty in light of variance errors. Nevertheless, the identified stationary data was

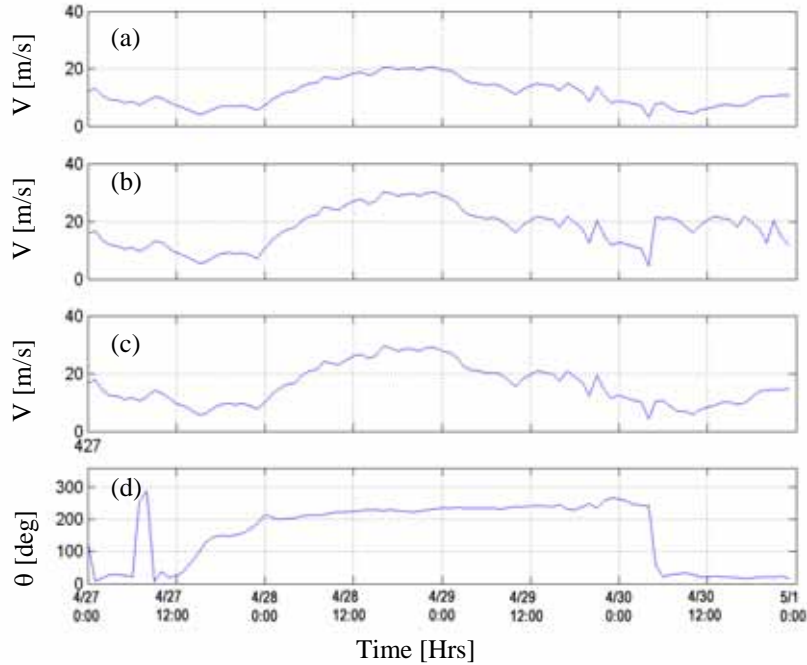


Figure 4. (a) NOAA GLERL surface level mean hourly wind speed; (b) gradient level mean hourly wind speed translated by Method 1; (c) gradient level mean hourly wind speed translated by Method 2; (d) NOAA GLERL surface level wind direction.

broken into segments of sufficient length so as to provide bias errors of less than -2% and then averaged to reduce variance as much as possible given the amount of data available.

Random Decrement Technique: The stationary response data was first pre-processed by Butterworth bandpass filters to isolate each mode of interest before applying the Random Decrement Technique. Once the RDS is obtained, it is fit using the Hilbert Transform to extract frequency and damping from the phase and amplitude of the analytic signal. Due to the sensitivity of trigger conditions on the number of segments captured, the reliability of the Random Decrement Technique can be improved through repeated triggering, as proposed in Kijewski-Correa [1]. This is accomplished by generating Random Decrement Signatures for positive point triggers that are multiples of the standard deviation of the acceleration response being analyzed ($X_p = M\sigma$). By restricting these triggers within a few percent of M , multiple RDS can be generated, from which frequency and damping values can be estimated and subsequently averaged for the mean estimate of the dynamic properties associated with a trigger of $M\sigma$ and their accompanying Coefficients of Variation (CoV).

Discussion: The period and damping estimates by the aforementioned spectral and time-domain approaches are presented in Table 3. These are compared to the design predictions shown previously in Table 2. For reference, the relative responses of x-sway, y-sway and torsion-induced lateral sway during this event were: 1:1.7:0.17 for Building 1, 1:0.52:0.05 for Building 2 and 1:0.76:0.12 for Building 3. This confirms the lack of torsional response in the buildings, as expected given their high torsional stiffnesses. Further, the behaviors of Buildings 2 and 3 show the amplified response in the E-W direction (x-sway), characteristic of a dominant acrosswind response for this wind event. This is not the case in Building 1, however, where the acrosswind axis (x-sway) is considerably stiffer (see Table 2), yielding a dominant alongwind response for this wind event.

Generally, excellent consistency between the two approaches is observed for period estimation. The exception is the torsional mode of Building 3, which still manifested evidence of coupling and thus difficult to filter and analyze by the RDT approach. The CoV for all the RDT analyses are well under 1%,

demonstrating the reliability with which periods are identified. In Building 1, in-situ periods of vibration show excellent agreement with the predictions in Table 2. Some slight discrepancy is noted between the HPBW and RDT results for Y-sway, which being a very long period response, provides fewer averages in both the spectral and RDT methods, as evidenced by its relatively higher CoV. Building 2 demonstrates periods 11-25% stiffer in-situ than predicted by the FE models. This may be attributed to the FE model's stiffness reductions due to cracking that has yet to be observed in the service life of this building. It is equally likely that the in-situ modulus of elasticity is larger than that assumed in the FE modeling. Building 3, on the other hand, has in-situ periods that are generally longer than FE model predictions, by approximately 10%. The causes of this in-situ behavior are currently being investigated.

As expected, the CoV of damping estimates by RDT are markedly higher than those of period estimates, reaffirming the difficulty in estimating damping. In addition to the CoV, the number of raw spectra averaged in the power spectral estimates is provided in Table 3 to give an indication of the variance errors. Again bias was first minimized to under -2%, but this leaves potentially high variance errors for a limited amount of data. This is particularly relevant to the spectral damping estimates for the longer period responses (Building 1 y-axis and Building 3 x & y-axes). However, the RDT results, which were generated from segments numbering in the thousands, likely provide a more reliable estimate of damping and showed consistency with the results in Kilpatrick et al. [8] for Building 1. Given that the return period of this event is approximately annual, and the assumed damping levels are intended for larger return periods, then the use of 1% damping in the design of these three buildings was likely appropriate for Building 1 and even conservative for Building 3. In the case of Building 2, the assumption of 1% seems highly conservative, as expected for a concrete structure.

Table 3. Periods of Vibration and Damping Ratios Estimated by Spectral and Time Domain Analyses for April 28, 2004 Wind Event.

		Building 1	Building 2	Building 3	Building 1	Building 2	Building 3
		Period [s]			Damping [percent critical]		
HPBW	X-Sway	4.89 (N=26)	5.62 (N=33)	8.60 (N=12)	0.65% (N=26)	1.62% (N=33)	1.46% (N=12)
	Y-Sway	7.06 (N=13)	5.65 (N=33)	8.62 (N=12)	1.14% (N=13)	2.07% (N=33)	1.06% (N=12)
	Torsion	1.99 (N=53)	3.41 (N=33)	4.48 (N=24)	0.74% (N=53)	3.14% (N=33)	1.31% (N=24)
RDT	X-Sway (COV)	4.89 (0.10%)	5.61 (0.22%)	8.60 (0.25%)	0.87% (23.9%)	1.42% (7.4%)	1.04% (20.6%)
	Y-Sway (COV)	7.11 (0.19%)	5.66 (0.68%)	8.60 (0.14%)	0.88% (8.9%)	2.4% (8.0%)	1.21% (23.0%)
	Torsion (COV)	1.99 (0.07%)	3.41 (0.71%)	4.35 (0.14%)	0.87% (14.9%)	3.59% (13.4%)	1.33% (16.9%)

Note: N indicates number of raw spectra in PSD average.

COMPARISONS TO WIND TUNNEL PREDICTIONS

A comparison of full-scale accelerations from Buildings 1, 2 and 3 with wind tunnel predictions is now presented. Torsional responses are not shown for brevity, since they are comparatively smaller. Note that at the design stage of a typical tall building, the inherent damping of a structure is rarely known with certainty, and estimates of the damping are made based on full-scale observations of similar structures. Given the potential variabilities in these and other critical parameters, upper and lower limits on predicted responses are presented here, based on the range of damping ratios that may be reasonably anticipated for

each building given the CoVs in Table 3, the periods of vibration observed in full-scale, and the range of wind directions recorded during the event. This suite of values is summarized in Table 4.

Table 4. Range of Wind Directions, Fundamental Periods and Damping Ratios Used in Wind Tunnel Predictions.

	Wind Direction	N-S Sway, Period (sec)	E-W Sway, Period (sec)	N-S Sway, Damping (%)	E-W Sway, Damping (%)
Building 1	230° – 250°	7.10	4.90	0.7 – 1.0	0.7 – 1.0
Building 2	230° – 250°	5.66	5.61	1.5 – 2.0	1.0 – 1.5
Building 3	230° – 250°	8.60	8.60	1.25 – 1.5	1.0 – 1.25

The measured and predicted RMS responses of Buildings 1-3 in the E-W and N-S direction are plotted against the estimated gradient wind speed in Figures 5-7, respectively. Note that although ultrasonic anemometers are now located above the rooftop of Building 3, they were not in place for this wind event. Thus, the wind speed data utilized here are extrapolated from NOAA met station measurements in accordance with the interim wind monitoring protocol. Also note that each building's RMS accelerations are normalized by the wind tunnel's predicted annual peak acceleration for that particular response component, to assess the quality of the predictions while preserving anonymity of the buildings' response magnitudes as per the agreements with the building owners. The measured full-scale data in Figures 5-7 correspond to the RMS accelerations recorded over 10-minute intervals by the data logger system from approximately 6:00PM on April 28th until 12:00PM April 29th during which time the estimated gradient wind direction was relatively stable from the West-Southwest. Note that the spread between upper and lower limits of response vary for each building and even each response direction due to the aerodynamic sensitivity of that particular building axis to wind direction and the inherent structural damping assumed in the analysis.

In Building 1, the wind tunnel predictions slightly underestimate E-W response, while overestimating N-S response. Agreement for Building 2 is generally very good and slightly conservative for the N-S response. Observed responses of Building 3 distribute rather uniformly about the predicted wind tunnel values. It is important to note that the NOAA wind speed and direction estimates are not exactly representative of conditions at each building, potentially explaining some of the observed scatter.

CONCLUDING REMARKS

This paper introduces a study established to allow the first systematic validation of tall building performance in the US using full-scale data in comparison with wind tunnel and finite element models used in design. For each of the three tall buildings currently monitored in the City of Chicago, instrumentation is overviewed and wind tunnel and analytical modeling approaches are summarized. A comparison of the full-scale response features with design predictions is provided for the April 28-29, 2004 wind event. Note that these efforts are presently being expanded for other observed wind events for a more comprehensive assessment of the design state-of-the-art.

ACKNOWLEDGEMENTS

The authors wish to gratefully acknowledge the support of the National Science Foundation through grant CMS 00-85109, UND, BLWTL, SOM, the Chicago Committee on High Rise Buildings, and Canada's Natural Sciences and Engineering Research Council, which supported the second author. The authors must also sincerely thank the building owners and management for their continued cooperation and enthusiasm, as well as students/engineers, technicians, legal counsel and support staff at UND, BLWTL and SOM for their efforts.

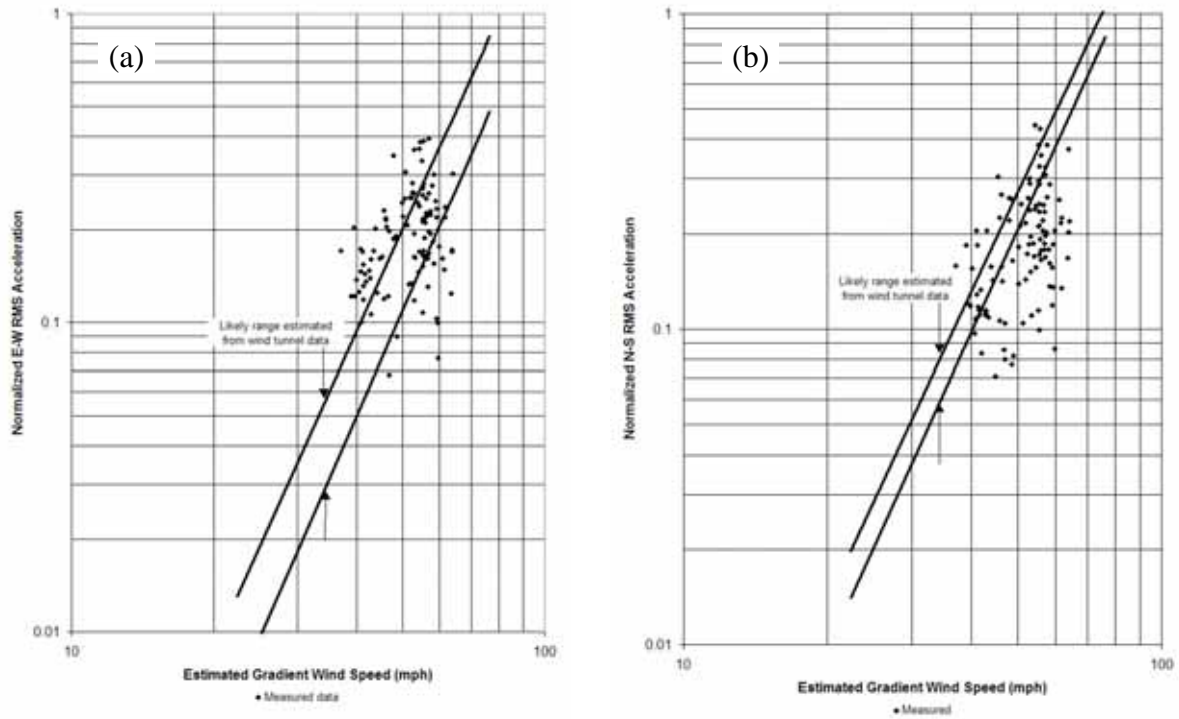


Figure 5. Building 1 - measured accelerations vs. wind tunnel predictions for (a) E-W and (b) N-S RMS sway response in April 28-29, 2004 wind event.

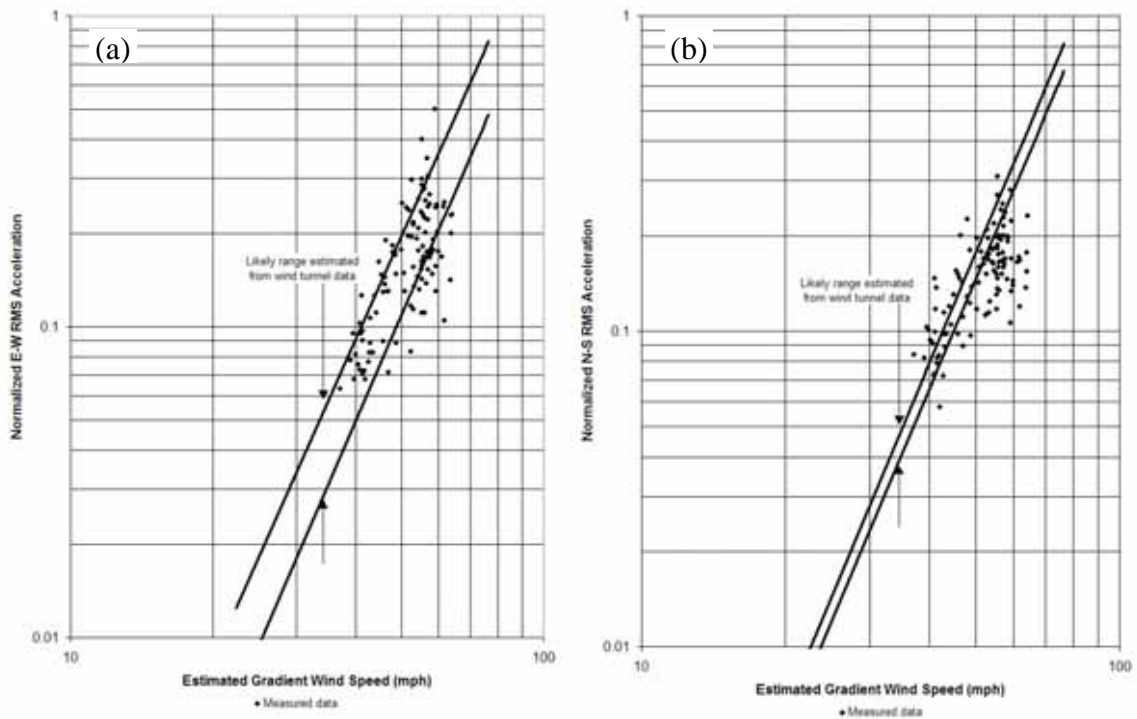


Figure 6. Building 2 - measured accelerations vs. wind tunnel predictions for (a) E-W and (b) N-S RMS sway response in April 28-29, 2004 wind event.

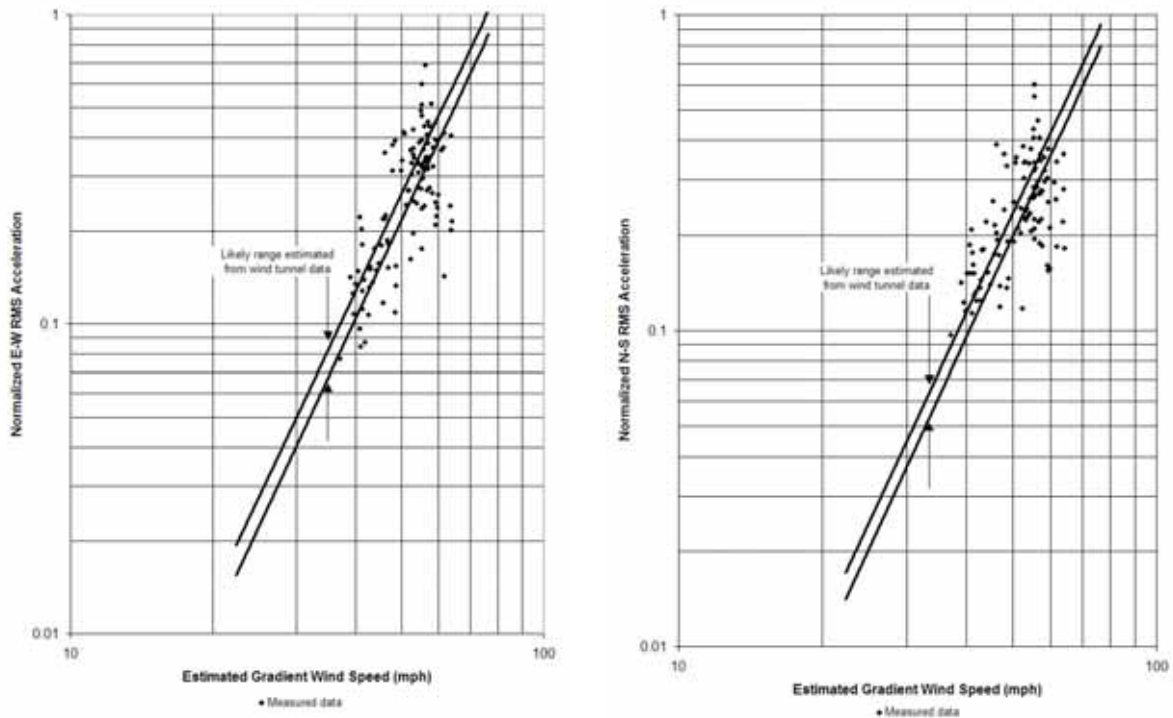


Figure 7. Building 3 - measured accelerations vs. wind tunnel predictions for (a) E-W and (b) N-S RMS sway response in April 28-29, 2004 wind event.

REFERENCES

- [1] T. Kijewski-Correa, Time-Frequency Perspectives in System Identification: From Theory to Full-Scale Measurements, PhD Dissertation, University of Notre Dame, Notre Dame, IN, 2003.
- [2] ESDU, Computer Program for Wind Speeds and Turbulence Properties: Flat or Hilly Sites in Terrain with Roughness Changes, Engineering Sciences Data Unit—01008, 2001.
- [3] P.J. Vickery, A. Steckley, N. Isyumov, B.J. Vickery, The effect of mode shape on the wind-induced response of tall buildings, 5th U.S. National Conference on Wind Engineering Proceedings, 1985.
- [4] X. Chen, A. Kareem, Coupled building response analysis using HFFB: some new insights, Proceedings of 5th International Colloquium on Bluff Body Aerodynamics and Applications, 2004.
- [5] ETABS, ETABS Version 8.0, Reference Manual, Computer & Structures, Inc., Berkeley, CA, 2002.
- [6] SAP, SAP 2002 Version 8.0, Reference Manual, Computer & Structures, Inc., Berkeley, CA, 2002.
- [7] F. Wachowski, Windiest spring since 1991: powerful wind gusts, Chicago Tribune, May 2, 2002.
- [8] J. Kilpatrick, T. Kijewski, T. Williams, D.K. Kwon, B. Young, A. Abdelrazaq, J. Galsworthy, D. Morrish, N. Isyumov, A. Kareem, Full scale validation of the predicted response of tall buildings: preliminary results of the Chicago monitoring project, 11th International Conference on Wind Engineering Proceedings, 2003.
- [9] ASCE, Minimum Design Loads for Buildings and Other Structures, SEI/ASCE7-02, American Society of Civil Engineers, Reston, VA, 2003.
- [10] J.S. Bendat and A.G. Piersol, Random Data: Analysis and Measurement Procedures, 2nd Ed, Wiley & Sons, New York, 1986.
- [11] H.A. Cole, On-Line Failure Detection and Damping Measurement of Aerospace Structures by Random Decrement Signatures, NASA CR-2205, 1976.
- [12] P.R. Montpelier, The Maximum Likelihood Method of Estimating Dynamic Properties of Structures, Master's Thesis, Department of Civil Engineering, University of Western Ontario, 1996.